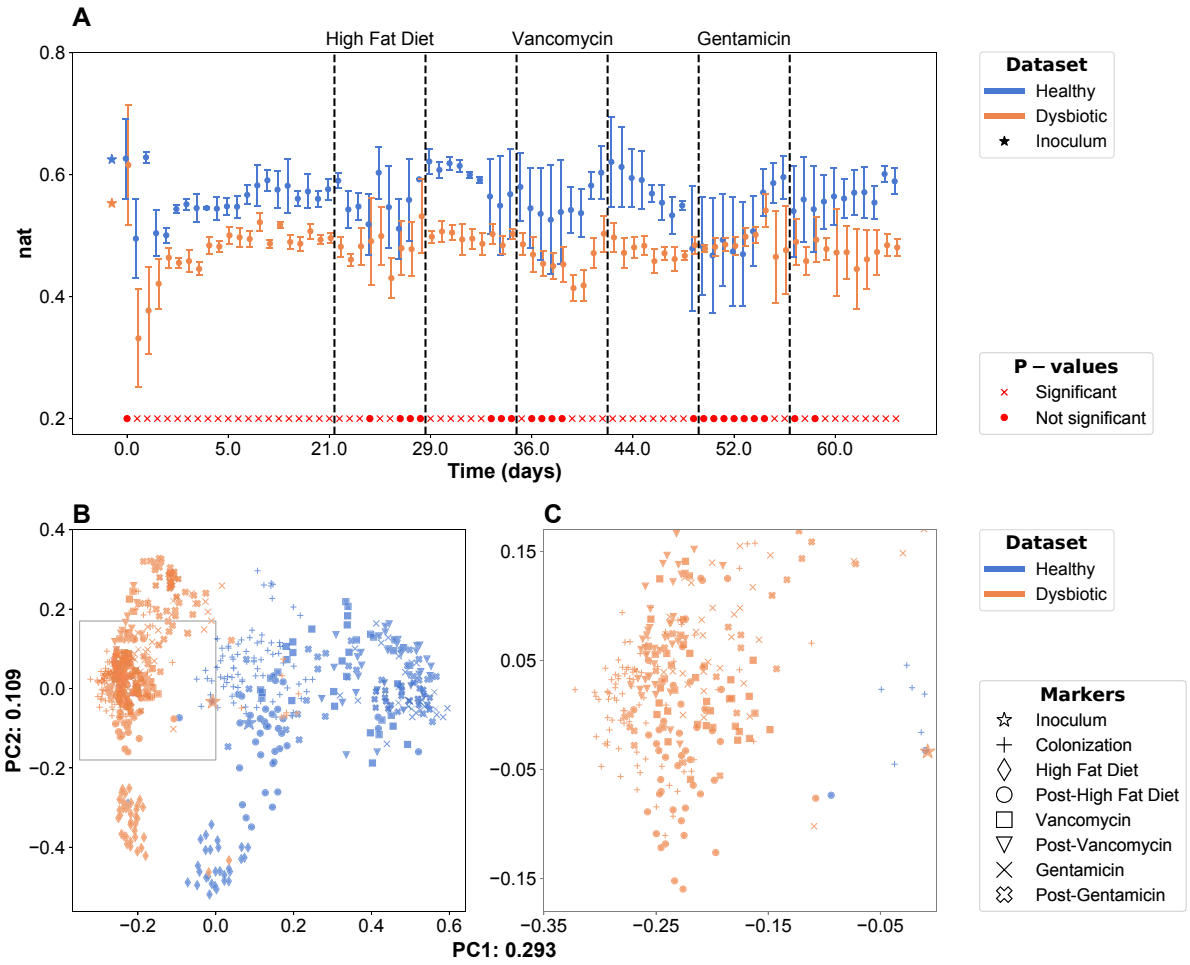

Supplemental Figure 1: Microbiomes from healthy donors maintain ecological diversity over time while remaining ecologically distinct from microbiomes from dysbiotic donors. (A) Alpha diversity (normalized Shannon entropy) for healthy and dysbiotic cohorts. Significance was assessed using the Wilcoxon rank-sum test and Benjamini-Hochberg correction. Mean and standard deviation are displayed for each time point. Stars indicate the diversity of the starting inocula. **(B)** PCoA plot of beta diversity (Bray-Curtis measure). **(C)** Zoom in from **(B)** (grey rectangle) showing that the dysbiotic donor cohort has less ecological diversity than the healthy donor cohort. Beta diversity between the two cohorts was significantly different (p=0.001, PERMANOVA test).

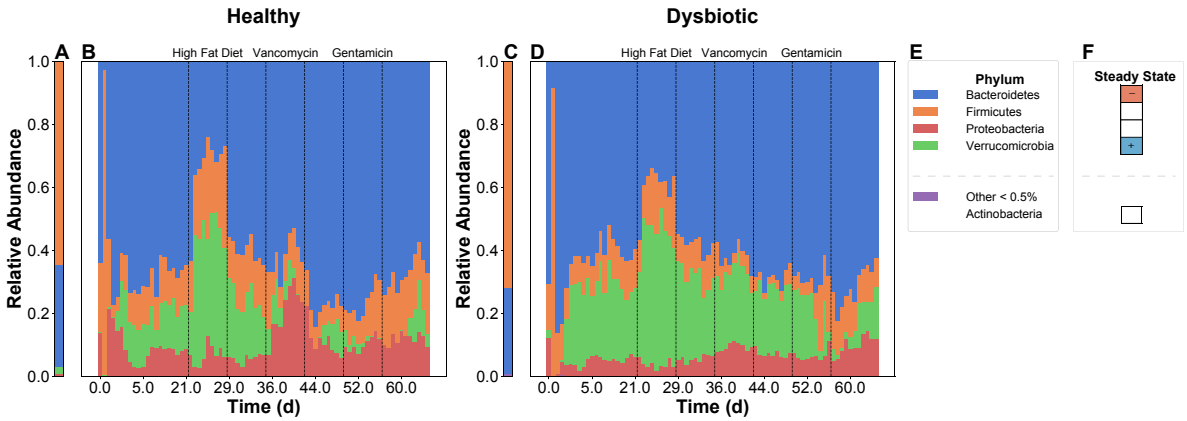

Supplemental Figure 2: Relative abundance of OTUs in healthy and dysbiotic donor microbiomes at the phylum level. (A) Relative abundance of microbes in starting inoculum from the healthy donor. **(B)** Relative abundances of microbes in serial fecal samples from mouse cohort receiving healthy donor microbiome, averaged over the biological replicates. **(C)**, **(D)** corresponding data from mouse cohort receiving dysbiotic donor microbiome. **(E)** Legend for figures (A), (B), (C), and(D). **(F)** Significant fold changes in sequencing counts at the phylum level (see Supp Table 2 for *p*-values).

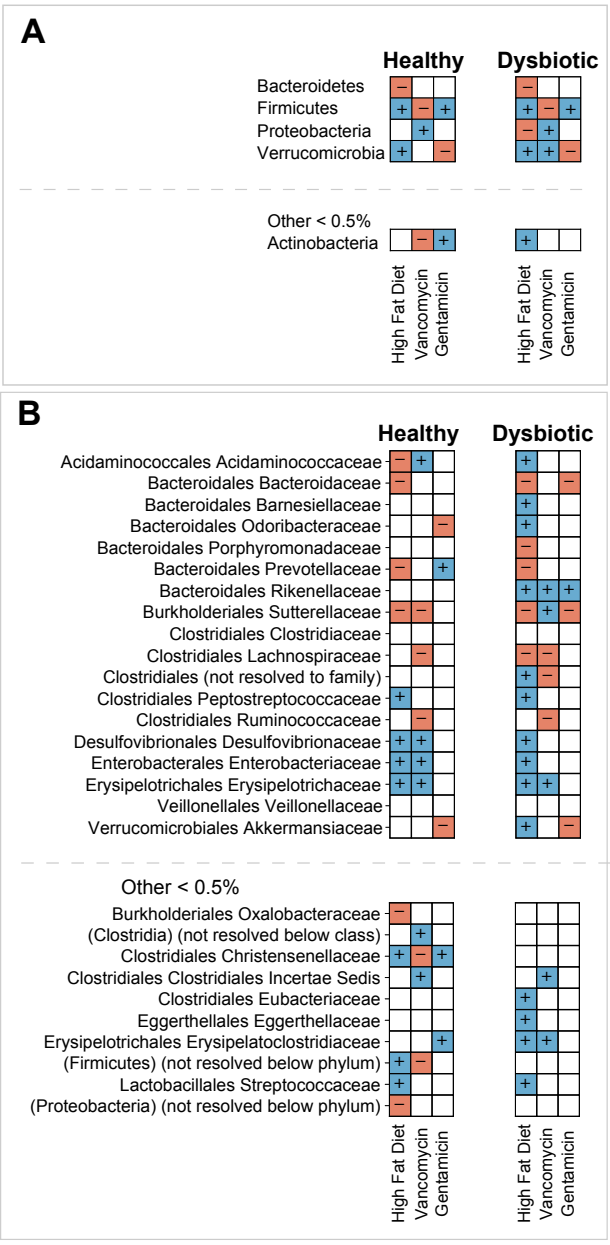

Supplemental Figure 3: Fold change analysis for perturbation responses at phylum and family levels. (A) Significant fold changes for the three perturbations at the phylum level (see Sup Table 2 for *p*-values). **(B)** Significant fold changes for the three perturbations at the family level (see Sup Table 2 for *p*-values).

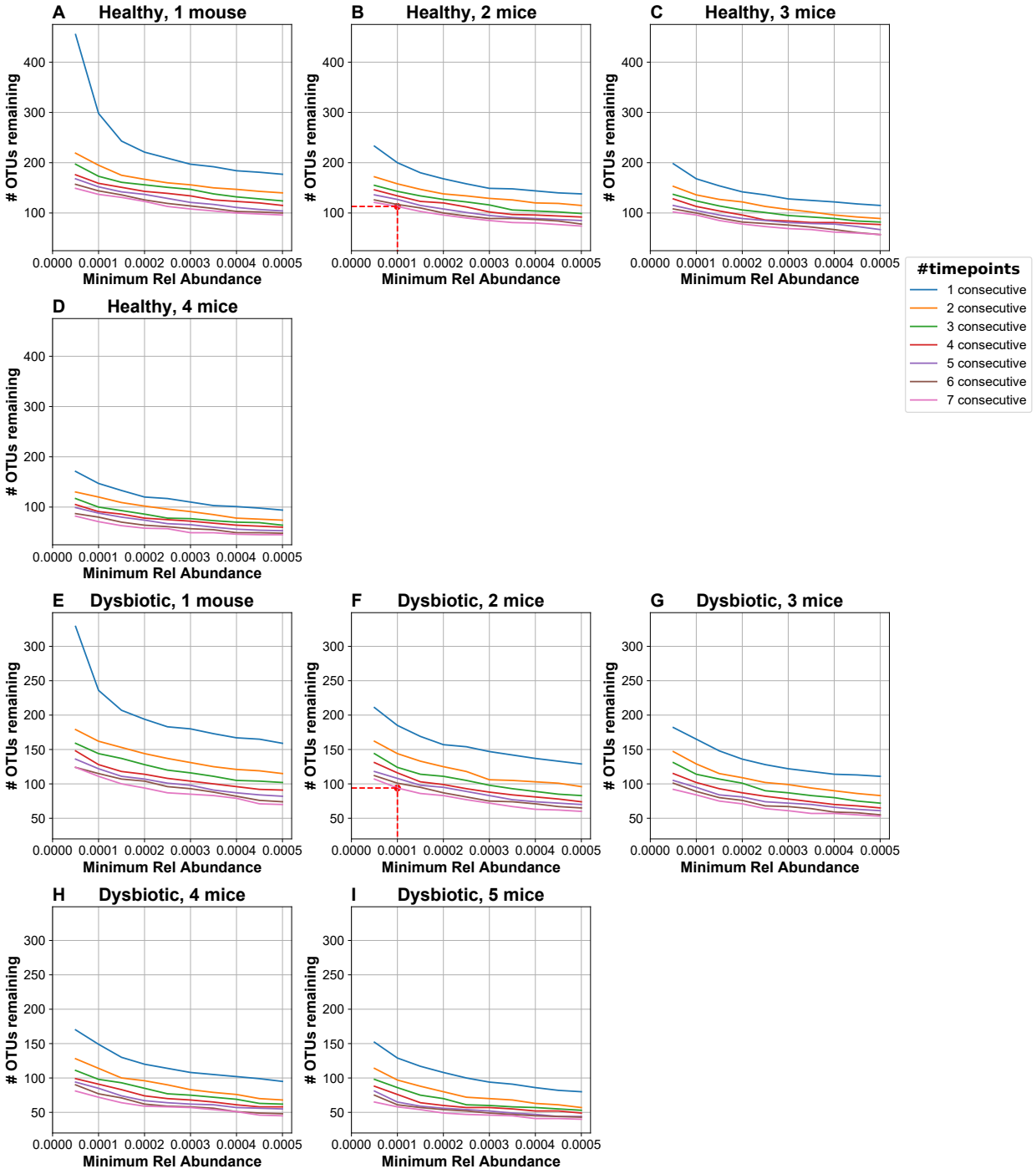

Supplemental Figure. 4: Filtering criteria for excluding rare and inconsistently colonizing OTUs. Plots show how many OTUs (y-axis) pass the initial filtering criteria for both healthy and dysbiotic donor microbiomes with varying parameters. To pass initial filtering, OTUs must have achieve a minimum relative abundance of X for Y consecutive timepoints in at least Z subjects after colonization. The filtering allows us to only keep OTUs that have rich dynamical information for inference. We set X, Y, and Z to 0.01%, 7, and 2 respectively, for analyses in this study. These settings and the corresponding number of OTUs that pass the filter are denoted by the red-dashed lines.

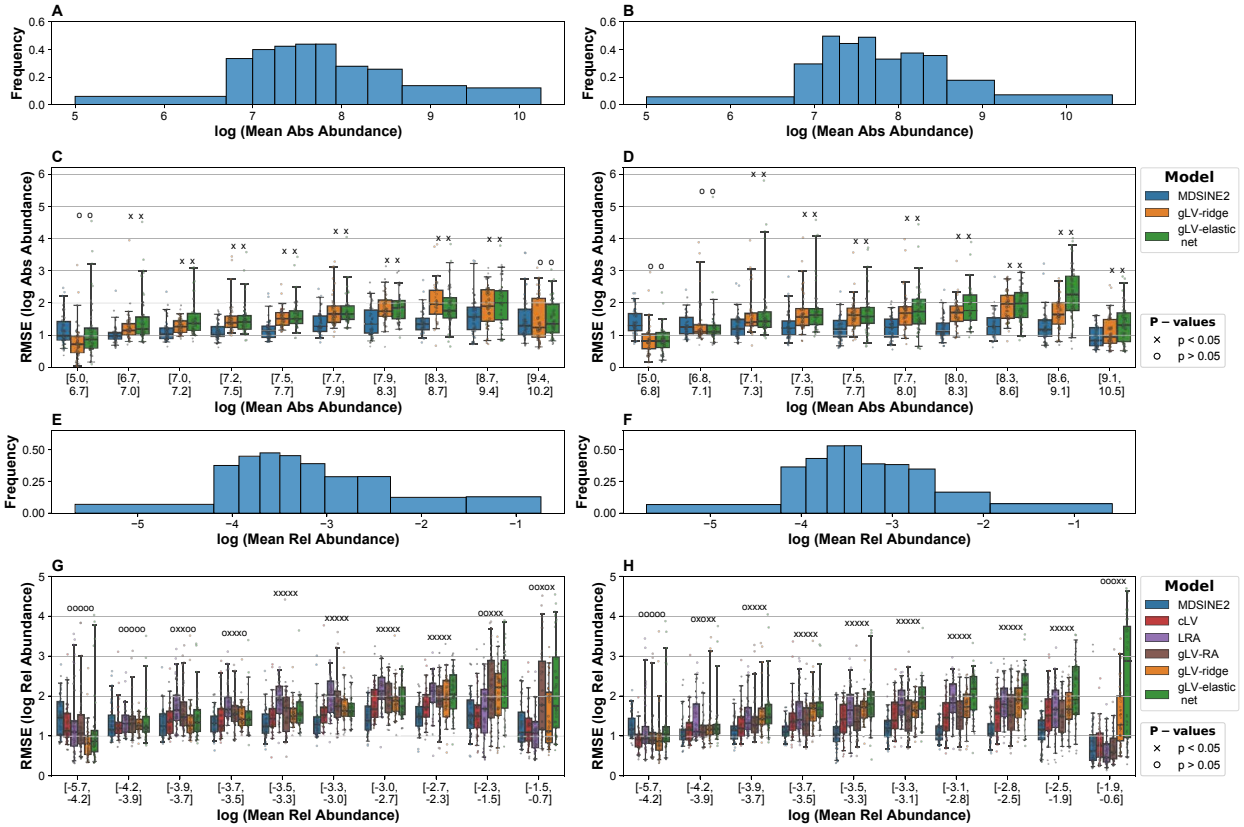

Supplementary Figure 5: MDSINE2 exhibits higher predictive performance for a wide range of relative and absolute abundances in comparison to state-of-the-art methods. Predictive performances were evaluated using Root Mean Square Error (RMSE) on forecasted trajectories with hold-one-subject-out cross validation. The significance of difference in RMSE between MDSINE2 and comparator methods was tested using the Signed-Rank Test followed by the Benjamini-Hochberg procedure for multiple comparison correction. MDSINE2, generalized Lotka-Voltera (gLV) with ridge (gLV-ridge) and elastic net regression (gLV-elastic) forecast trajectories in absolute abundance space. Compositional gLV (cLV), Linear Dynamics Relative Abundance (LRA), and gLV trained on relative abundance (gLV-RA) forecast relative abundances. **(A)** Histogram of the mean absolute abundances of OTUs in the healthy donor microbiome. Each bin contains approximately 10% of the total data. **(C)** Box plot showing absolute abundance RMSE of OTUs grouped according to the binning in (A). **(E)** Histogram of the mean relative abundances of OTUs in the healthy donor microbiome. Each bin contains approximately 10 % of the total data. **(G)** Box plot showing relative abundance RMSE of OTUs grouped according to the binning in (E). **(B)**, **(D)**, **(F)**, **(H)** corresponding plots for dysbiotic donor microbiome.

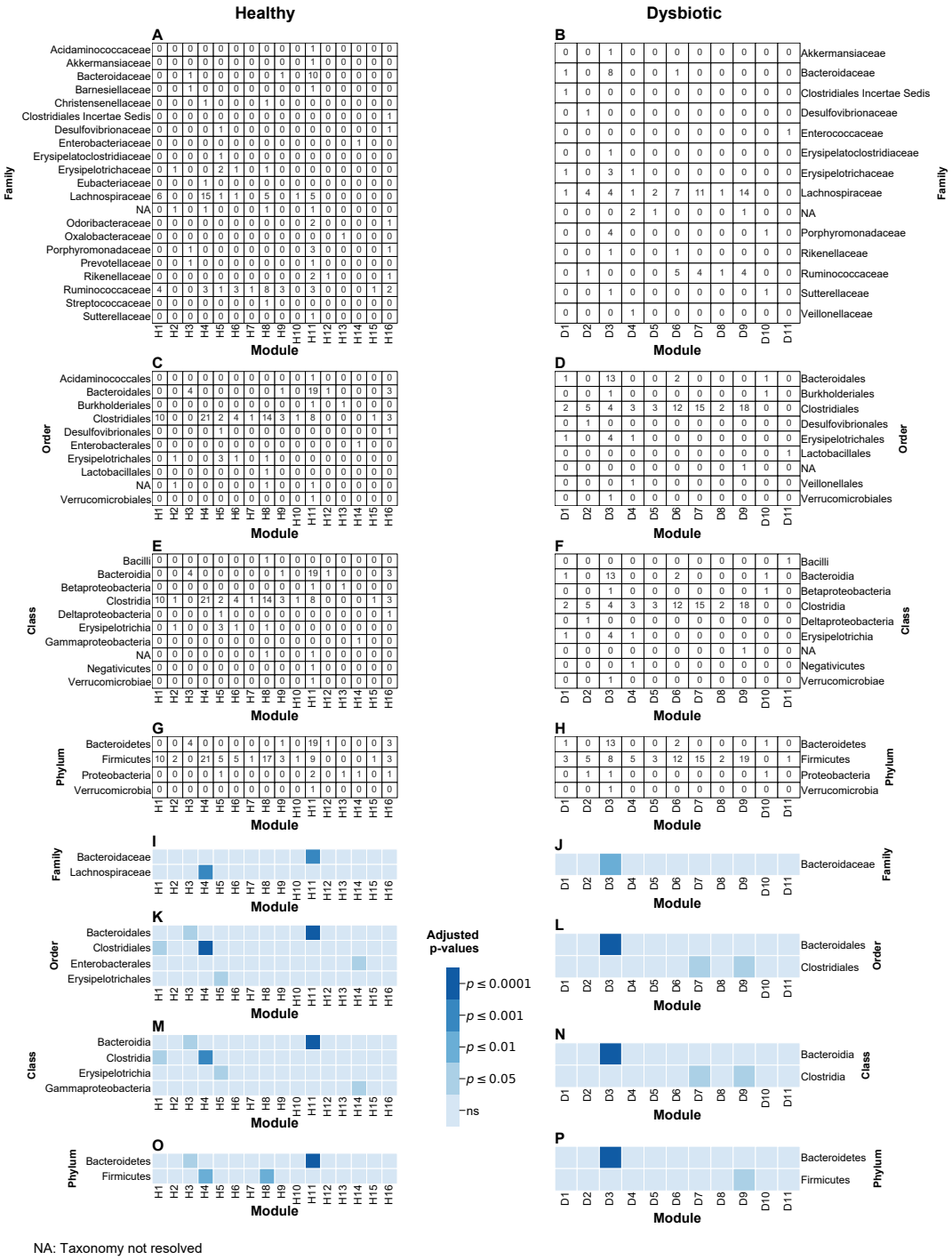

NA: Taxonomy not resolved

Supplemental Figure 6: Interaction modules were significantly enriched for OTUs at the family, order, class, and phylum taxonomic ranks. (A), (C), (E), and **(G)** display the number of OTUs in each module for the healthy donor microbiome at each taxonomic rank, and **(B), (D), (F),** and **(H)** display the corresponding information for the dysbiotic donor microbiome. **(I), (K), (M),** and **(O)** display which taxonomic labels were significantly enriched for each module in the healthy donor microbiome, and **(J), (L), (N)** and **(P)** display the corresponding information for the dysbiotic donor microbiome. Enrichment analyses were performed using the hypergeometric test with Benjamini-Hochberg correction for multiple comparisons.

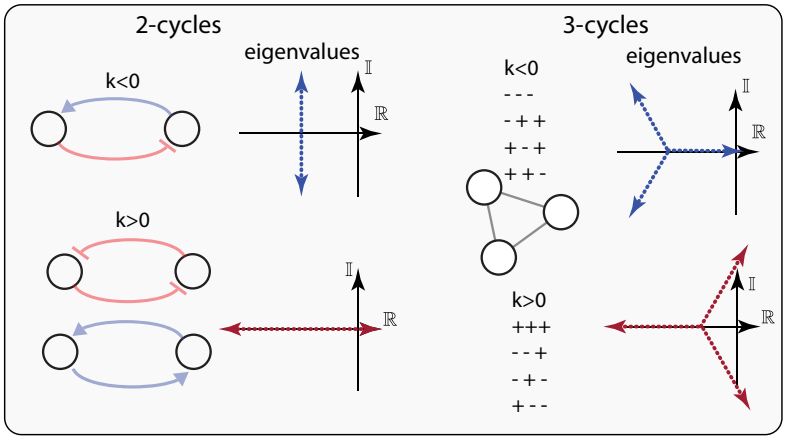

Supplemental Figure 7: Root locus of 2- and 3-cycles showing asymptotes of their eigenvalues. Only two cycles with negative feedback are stable for all cycle strengths. All other cycles can become unstable with strong enough interactions.